



RESEARCH ARTICLE

NUMERICAL ANALYSIS OF THE EFFECTS OF WINGLET SHAPES ON WING PERFORMANCE

1,\*Mohamed A. Khalifa, 2Abdelmotleb Ali Mostafa and 3Osama Ezzat Abdellatif

1PhD student, Teaching Assistant, Institute of Aviation Engineering & Technology, Giza, Egypt

2Professor, Mechanical Power Department, Cairo University, Egypt

3Professor, Mechanical Power Department, Benha University, Egypt

ARTICLE INFO

Article History:

Received 26<sup>th</sup> October, 2016  
Received in revised form  
15<sup>th</sup> November, 2016  
Accepted 15<sup>th</sup> December, 2016  
Published online 31<sup>st</sup> January, 2017

Key words:

CFD Simulation,  
Sharp Edge Winglet,  
Blended Winglet,  
Lift to Drag Ratio.

ABSTRACT

This study presents CFD 3-D winglets analysis on a civil aircraft wing of NACA23016 airfoil for root wing section, NACA 23014 airfoil for mean wing section and NACA 23012 airfoil for tip wing section. These airfoils were considered as 4 m chord length at root section, 2.8 m chord length at mean section and 1.6 m chord length at tip wing section at which is added the winglet with the same profile at tip section with 45 degree cant angle. A CFD study to evaluate the aerodynamics characteristics of lift coefficient CL, drag coefficient CD and lift to drag ratio, L/D lift, pathlines and pressure contours is presented. All wings are simulated at a subsonic Mach number of (0.2) and ambient conditions pressure of (1 bar) and temperature of (15o C) at sea level. The wing with winglet blended connection has approximately the lift to drag ratio, CL/CD range varies from (11- 12.4)% with different air stream angles more than wing without winglet. The wing model with sharp edge winglet has lift to drag ratio, CL/CD range varies from (6.4- 8.2) % with different air stream angles less than the wing without winglet. CFD results proved that the wing with blended winglet is more efficient than the wing with sharp edge.

Copyright©2017, Mohamed A. Khalifa et al. This is an open access article distributed under the Creative Commons Attribution License, which permits unrestricted use, distribution, and reproduction in any medium, provided the original work is properly cited.

Citation: Mohamed A. Khalifa, Abdelmotleb Ali Mostafa and Osama Ezzat Abdellatif. 2017. "Numerical Analysis of the Effects of Winglet Shapes on Wing Performance", International Journal of Current Research, 9, (01), 44643-44649.

INTRODUCTION

Tip vortices are major problem in aircraft conditions, which increase drag on the aircraft wing. Drag is a phenomenon needs to be solved, specially induced drag. To avoid this phenomenon of drag, tip fences and winglets are used to decrease fuel consumption, improve aircraft performance, caring in air traffic control and decrease tip vortices. Winglet is mechanism attached to the wing tip. Winglet use to decrease fuel consumption, improves aircraft performance, and decrease tip vortices. Kubrynski, (2013) presented optimization approach for a multi-shape design which actually resulted in elevated sailplanes performance with blended winglets. Minella, et al. (2010) investigated different configurations of winglets by using 3-D aerodynamic analysis. It found that blended winglet has better performance than split winglet shape. Nikola et al. (2014) studied the effects of winglets on aircraft performance. Five configurations of winglets investigated numerically to evaluate the aerodynamic performance using multi-objective optimization software techniques to obtain one of the optimal configurations of winglet that is decreasing drag and increasing lift. Figure 1 shows Aircraft wing geometry considered in present paper a 50-passenger (CRJ – 100) aircraft wing with sharp edge and blended

wing let, wing of NACA23016 airfoil for root wing section, NACA 23014 airfoil for mean wing section and NACA 23012 air foil for tip wing section. These airfoils were considered as 4 m chord length at root section, 2.8 m chord length at mean section and 1.6 m chord length at tip section.

Governing Equations

Aircraft wing model is subjected to air flow considered as compressible viscous flow in 3-D. Air flow velocity and density are related in the continuity equation associated with Navier-Stokes equations. These differential forms of governing equations for compressible flow are presented here. Spalart-Allmaras model is chosen from turbulence modelled. Here the FLUENT® Manuel (Versteeg, 1995) & (FLUENT Documentation, 2005) is presented in differential form of the model governing equations.

- Continuity equation:  $\frac{\partial \rho}{\partial t} + \nabla \cdot (\rho \vec{V}) = 0$
- Momentum equation:  $\nabla \cdot (\rho \vec{V} \vec{V}) = -\nabla p + \nabla \cdot (\vec{\tau}) + \vec{F}$
- Energy equation:  
 $\frac{\partial(\rho E)}{\partial t} + \nabla \cdot (\rho \vec{V}(\rho E + p)) = \nabla \cdot [k_{eff} \nabla T - \sum_j h_j J_j + (\vec{\tau}_{eff} \cdot \vec{V})] + S_e$

CFD Verification

A numerical model for rectangular wing with NACA 653218 geometry is generated with its mesh by Ansys (15) and

\*Corresponding author: Mohamed A. Khalifa,  
PhD student, Teaching Assistant, Institute of Aviation Engineering & Technology, Giza, Egypt.

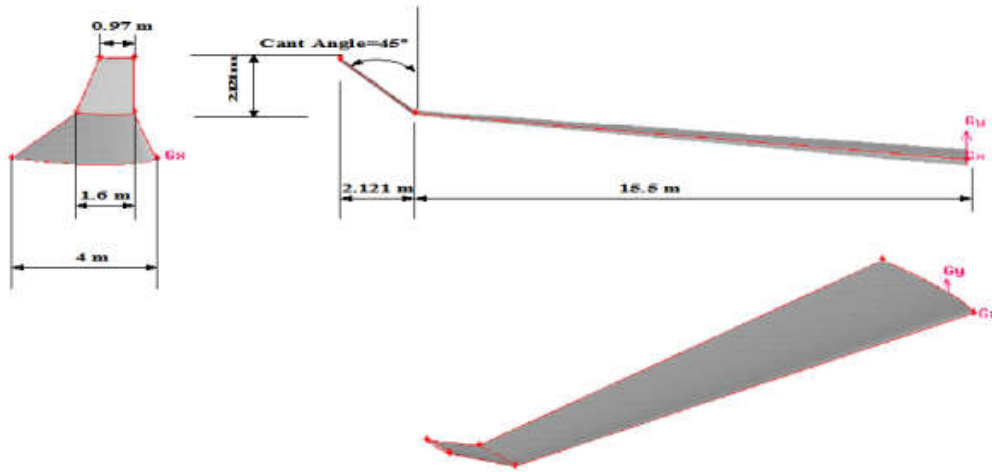


Figure 1-a. Aircraft wing with sharp edge winglet 45 cant angle (Abdelghany et al., 2016)

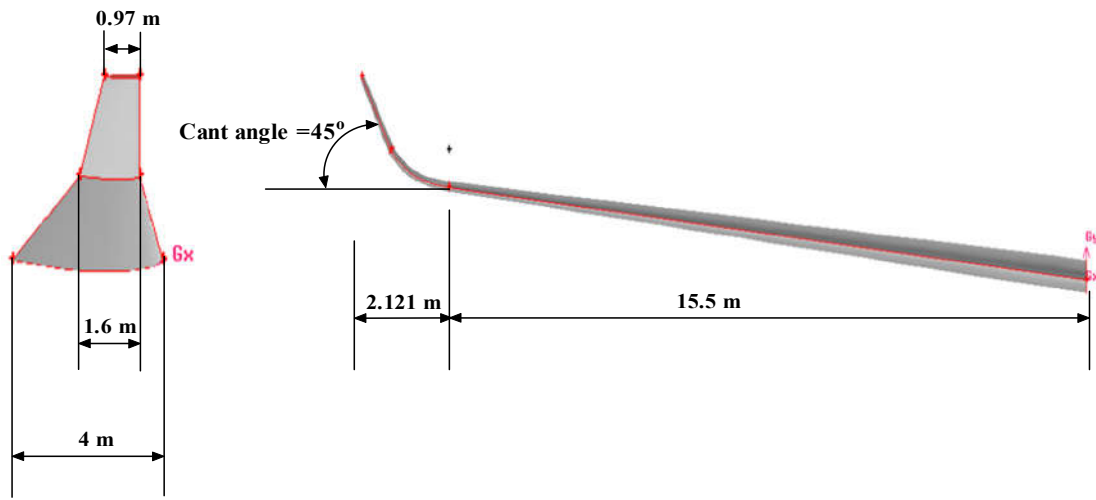


Figure 1. b. Aircraft wing with blended winglet 45 cant angle (Abdelghany et al., 2016).

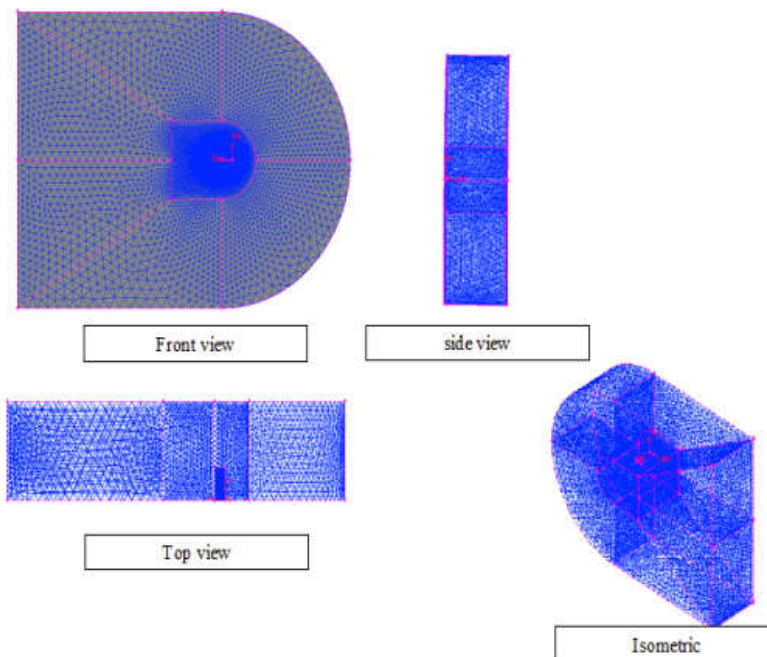


Figure 2. Wing control volume mesh

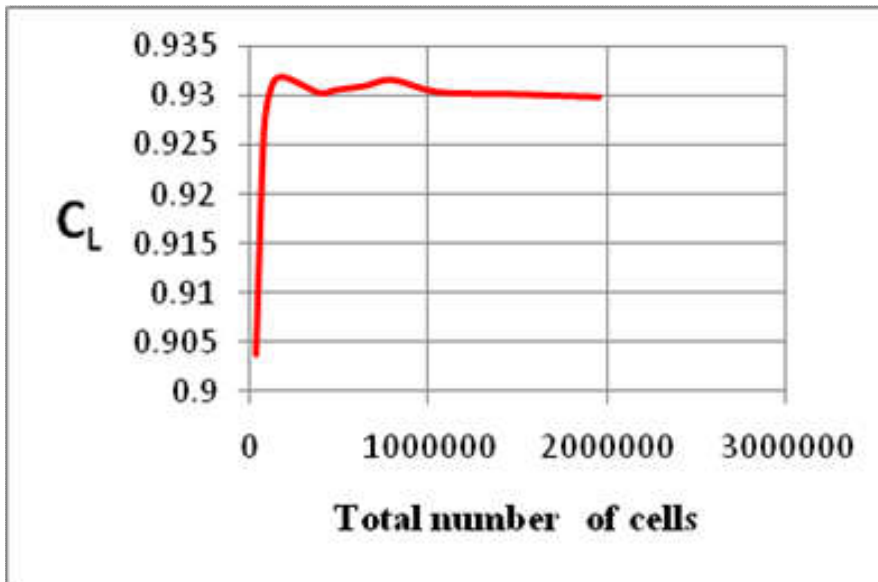


Figure 3. lift coefficient of fair stream angle,  $\alpha=12$  degree VS number of grid



Figure 4. The distribution of the Coefficient of lift against air stream angle ( $\alpha$ ), for different wing shapes

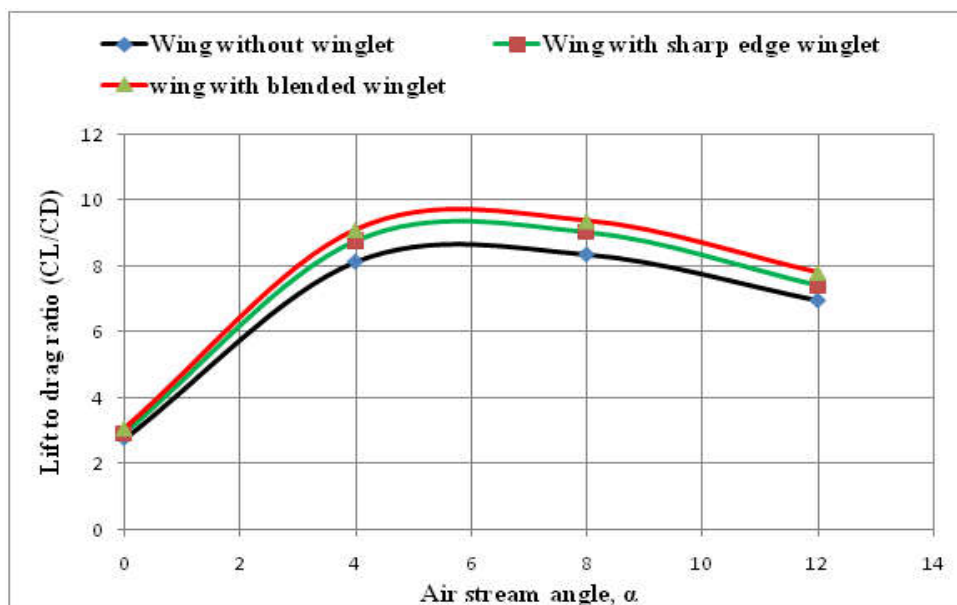


Figure 5. The distribution of CL/CD ratio against angle attack ( $\alpha$ )

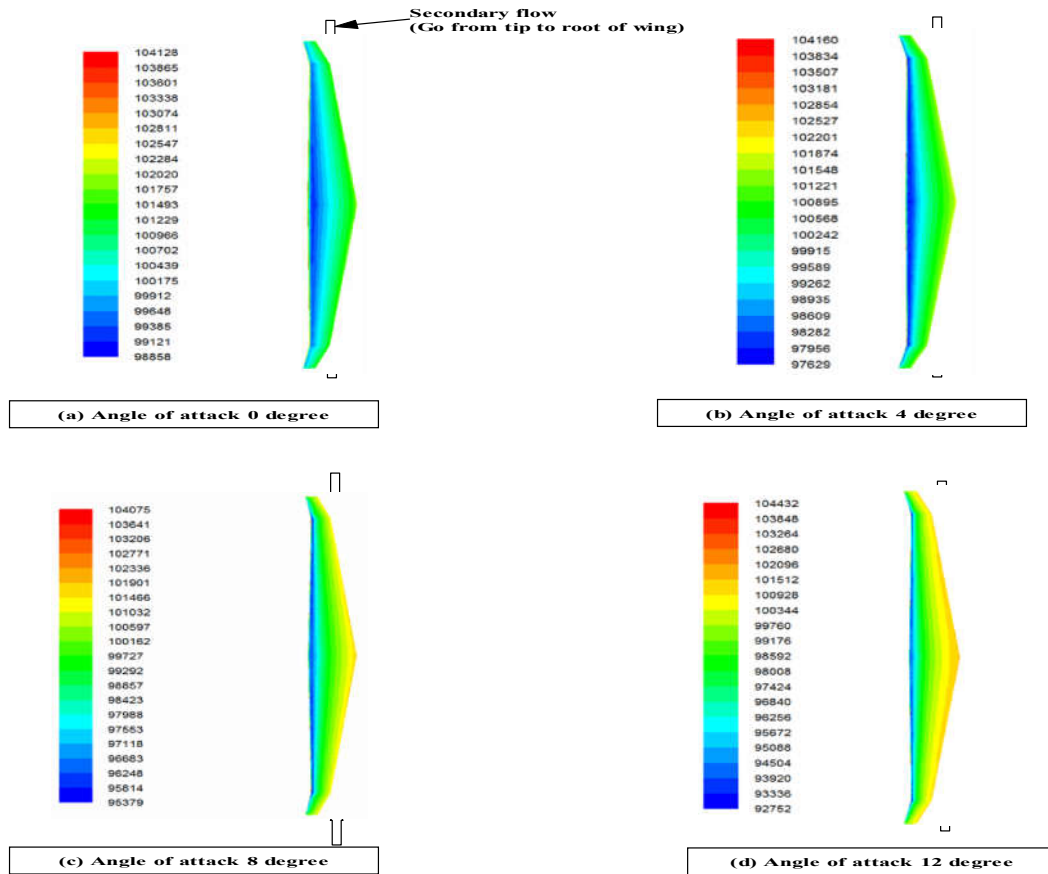


Figure 6a. Wing with sharp edge winglet pressure contours

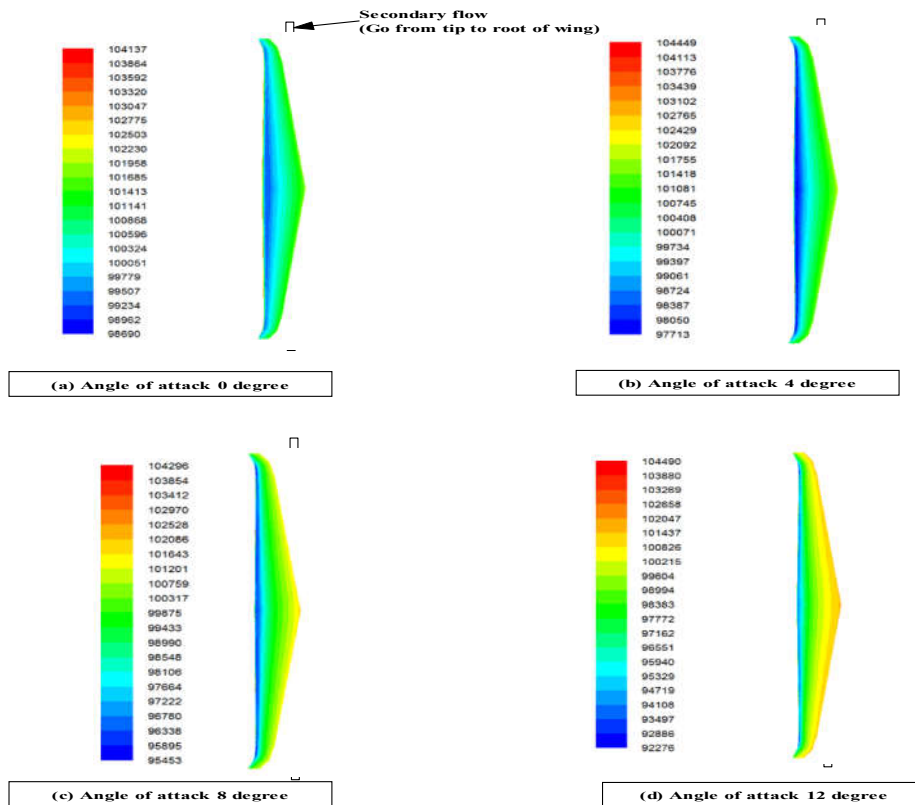


Figure 6 b. Wing with blended winglet pressure contours

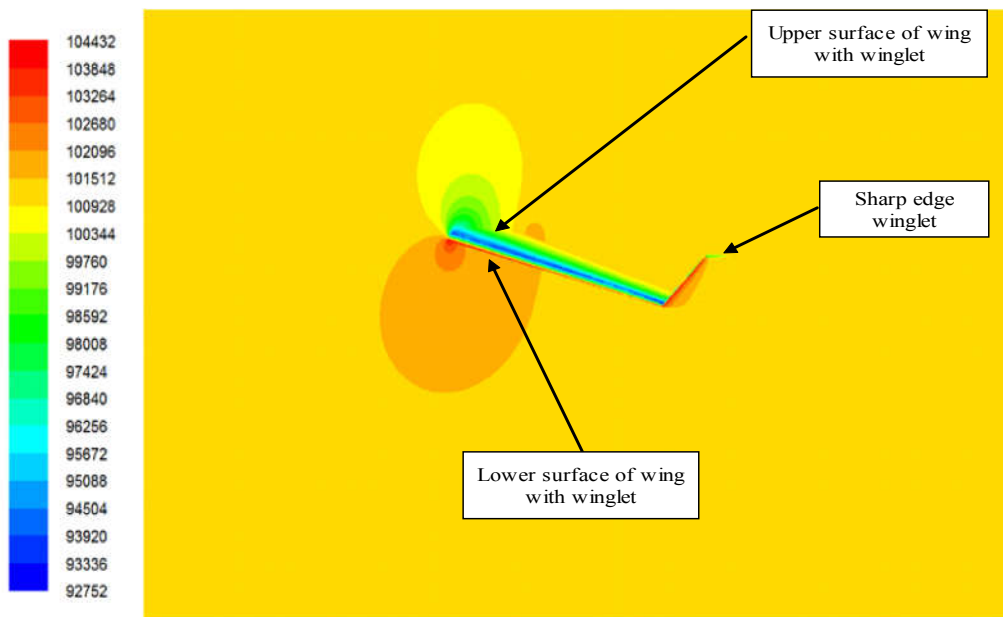


Figure 7a. Aircraft semi-span wing with sharp edge winglet pressure contour of a CRJ - 100 with cant angle 45 degree isometric view at Air stream angle,  $\alpha=12$  degree.

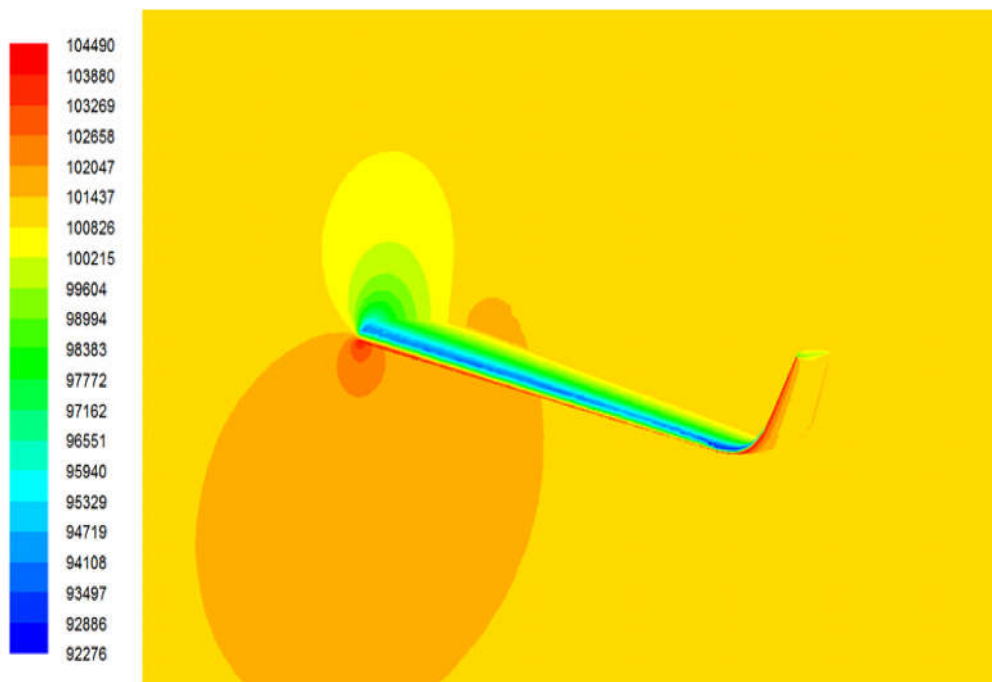


Figure 7b. Aircraft semi-span wing with blended winglet pressure contour of a CRJ - 100 with cant angle 45 degree isometric view at Air stream angle,  $\alpha=12$  degree

subjected to ambient conditions of 1-bar Pressure and temperature of 288-K at subsonic Mach No of 0.2 then solved by FLUENT software using finite volume method. Results obtained are aerodynamics characteristics like lift, Drag at different air stream angle ( $\alpha$ ), also Path lines on the wing.

**Geometry and Grids**

Atapered wing with NACA23016airfoil for root wing section, NACA23014 airfoil for mean wing section and, NACA23012 airfoil for tip wing section of A CRJ - 100 aircraft wing are considered. The airfoils are drawn using Gambit with a chord length of 4 m at root section, a chord length of 2.8 m at mean section and a chord length of 1.6 m at tip section.

The wing has a span of 31m. In order to achieve lift and drag on wing, GAMBIT® software is generated mesh, which close to the wing volume should be small enough to satisfy boundary conditions for far field (Abdelghany *et al.*, 2016). Tetrahedral unstructured mesh used for complex shape of winglet. Near to the wing wall size of grid must be small enough to reach to the good results of lift and drag. Figure 2 shows also the grid volumes important used to reduce time of solution and owed memory.

**Grid independency check**

In general, a numerical result becomes exact by increasing number of cells.

When the computations running, aimed to save time, the minimum cells number demonstrate grid independency check for the calculations presented. In the present study grid sizes of  $0.5 \times 10^6$  to  $2 \times 10^6$  by step of  $0.5 \times 10^6$  are used and the  $C_L$ . The lift coefficient at the air stream angle is monitored as shown in figure 3. It is clear for that figure that to be considered. These cases for a grid with around 1,500,000 cells as a reasonable grid size to produce grid independent solution.

**RESULTS AND DISCUSSION**

In this section the results obtained from CFD calculation for lift coefficient, drag coefficient, path lines and pressure contours around wing at different air stream angles are presented.

**Aerodynamic Analysis**

Figure 4 shows lift coefficient, increase with increase in air stream angle,  $\alpha$ . This figure also shows that, wing with blended winglet has the highest lift coefficient,  $C_L$ , ranges from 13.6% to 14.5% with air stream angle comparing with the wing without winglet. The wing with sharp edge winglet gives the next highest lift coefficient,  $C_L$ , ranges from 10% to 11.6% with air stream angle comparing with the wing without winglet. Figure 5 shown below; indicates that the wing with blended winglet has maximum lift to drag ratio;  $C_L/C_D$  by about 11% to 12.4% with different air stream angles comparing with the wing without winglet. Trends is followed by wing with sharp edge winglet, which is the next highest lift to drag ratio where  $C_L/C_D$  range from 6.4% to 8.2 % with different air stream angles comparing with the wing without winglet.

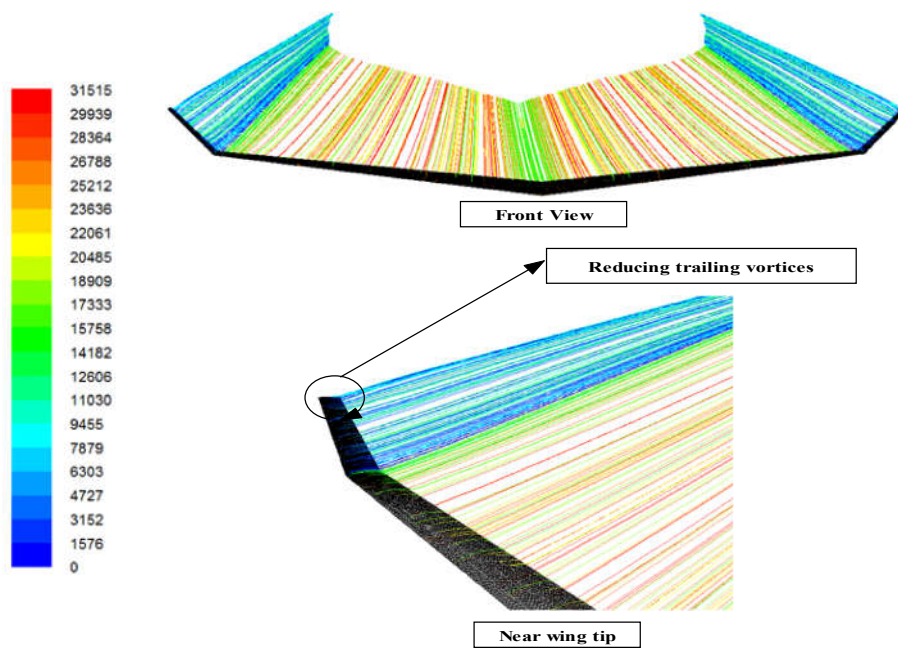


Figure 8a. Wing with sharp edge winglet pathlines at air stream angle,  $\alpha=12$  degree

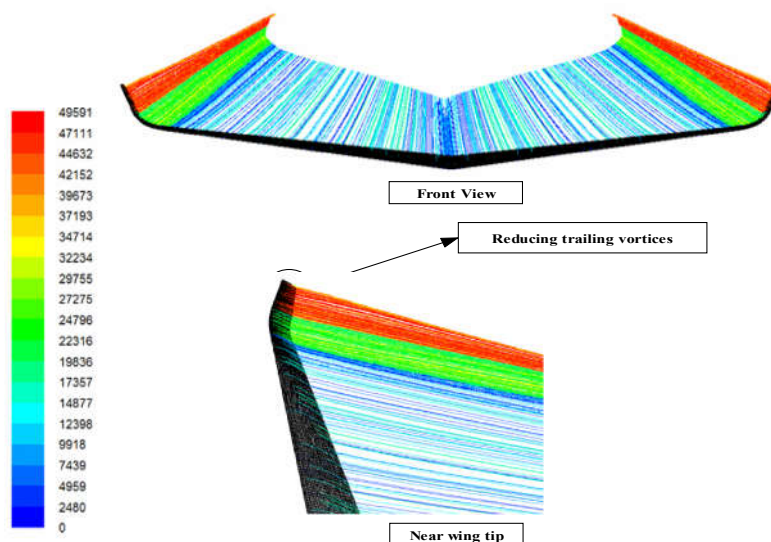


Figure 8b. Wing with blended winglets pathlines in case at air stream angle 12 degree

## Pressure Contours

Figure 6 shows upper static pressure contours for wing with winglet at cant angle, 45 degree. At air stream angle 0 degree, the minimum static pressure is located at the upper surface. At air stream angle,  $\alpha=12$  degree, the high intensity blue area are located on the upper surface. The figure also shows that the contours of the most of the total force are directed backward as drag. For all air stream angles, the minimum static pressure zones are located at mid of the wing. The figure also shows that minimum pressure value is higher than the minimum pressure value at the root. The r pressure decreases from root to tip, then the pressure increases to reach the atmosphere pressure, so as to reducing vortices at wing tip.

## Effects of different winglets with cant angle 45°

Figure 7 show pressure contours on sides of the wing surface with blended winglets, for different angles of attack. These wings with different winglets tested at a subsonic Mach number of 0.2 and ambient conditions pressure of (1 bar) and temperature of (288 K) at sea level.

## Pathlines

It is well-known that pressure difference between both sides of wing surfaces of makes vortices. When pressure difference increase with increasing of air stream angle then wing vortex is increasing. The wing with blended winglet and wing with sharp edge actually reduce vortices at the wingtip as expected. The rotational motion can be visualized more easily by presented the path lines. The path lines indicate that fluid is moves from lower to upper surface thus creating vortices. Figure 8 shows path lines over the wing with winglet at maximum air stream angle of 12°. Path lines are zoomed in at the wingtip where trailing vortices occurs. Due to the small e in pressure difference between both sides of wing surfaces tip vortices are very small

## Conclusion

Winglet designs considerably yield improvement of the aircraft performance and fuel consumption reduction. Effects of blended winglet and sharp edge winglet were investigated using CFD technique. In addition, to comparisons between the blended winglet, sharp edge winglet and the case without winglet. Each case was compared to cases without winglet, with the sharp edge winglet and blended winglet. The wing with winglet blended connection has lift to drag ratio, CL/CD range varies from (11- 12.4) % with different air stream angles more than wing without winglet. The wing model with sharp edge winglet has lift to drag ratio, CL/CD range varies from (6.4- 8.2) % with different air stream angles less than the wing without winglet at air stream angle  $\alpha=6$  degree.

## Nomenclature

b	:Wing span
C	:Chord length
$C_L$	:Lift coefficient
$C_D$	:Drag coefficient
E	:Total fluid energy
h	:Enthalpy
t	:Time
$\alpha$	:Air stream angle
T	:Temperature
M	:Mach number
S	:Wing area
P	:Pressure value
Re	:Reynolds number, $Re = U C / \nu$
$\nu$	:Kinematic viscosity
$S_h$	:Source term
$\rho$	:Density
$\alpha$	:Air stream angle
F	:External body forces

## REFERENCES

- Abdelghany, E. S., Khalil, E. E., Abdelatif, O. E. and Elharriry, G. M. 2016. "Aircraft Winglet Design and performance: Cant angle effect", *Journal of Robotics and Mechanical Engineering Research*, vol. 1, issue 3, pp. 28-34.
- Azlin, M. A., Mat Taib, C. F., Kasolang, S and Muhammad, F. H. 2011. "CFD Analysis of Winglets at Low Subsonic Flow", *World Congress on Engineering*, Vol. 1, pp. 1-5, 2011.
- Bourdin, P., Gatto, A. and Friswell, M.I. 2006. The application of variable cant angle winglets for morphing aircraft control, *24th AIAA Applied Aerodynamics Conference, San Francisco, CA*, June 5-8.
- FLUENT Documentation. © Fluent Inc. 2005.
- Gavrilović Nikola, N., Rašuo Boško, P., Dulikravich George, S., Parezanović Vladimir, B. 2014. "Commercial Aircraft Performance Improvement Using Winglets, Computational Mechanics", 6th European Conference on Computational Fluid Dynamics, Barcelona, Spain, July 20-25.
- Kubrynski, K. 2003. "Wing-winglet design methodology for low speed applications", AIAA paper 03-0215, 41st Aerospace Science Meeting and Exhibit, Reno, NV, January.
- Minella, G., Ugas, A. and Rodriguez, Y. 2010. Aerodynamic shape design optimization of airplane winglets, Senior year B.Sc. thesis, MME Dept., Florida International University, Miami, FL, December.
- Robert, T., Jones, 1984. "Improving The Efficiency Of Smaller Transport Aircraft", 14th Congress of the International Council of the Aeronautical Sciences, *Proceedings, Vol. 1, Toulouse, Fr.*
- Versteeg, H., and Malalasekera, W. 1995. "An Introduction to Computational Fluid Dynamics: The Finite Volume Method" Longman.
- Weierman, J. and Jacob, D. 2010. "Winglet design and optimization for UAVs", *AIAA Applied Aerodynamics Conference*, June 28 - July 1.

\*\*\*\*\*